Observation of coherent electron transport in self-catalysed InAs and InAs$_{1-x}$Sb$_{x}$ nanowires grown on silicon

M. J. L. Sourribes, I. Isakov, M. Panfilova, and P. A. Warburton

Observation of coherent electron transport in self-catalysed InAs and InAs$_{1-x}$Sb$_x$ nanowires grown on silicon

M. J. L. Sourribes, I. Isakov, M. Panfilova, and P. A. Warburton
London Centre for Nanotechnology, UCL, London, United Kingdom

We report the observation of phase coherent transport in catalyst-free InAs and InAs$_{1-x}$Sb$_x$ nanowires grown by molecular beam epitaxy on silicon (111) substrates. We investigate three different methods to gain information on the phase coherence length of the nanowires: first through the study of universal conductance fluctuations as a function of both magnetic field and gate voltage and then through localisation effects. The analysis of these different quantum effects gave consistent results and a phase-coherence length in the hundred nanometre range was extracted for all nanowires below 10 K. This demonstrates the potential of catalyst-free nanowires as building blocks for future quantum electronics devices directly integrated with silicon circuits. *Published by AIP Publishing.* [http://dx.doi.org/10.1063/1.4972960]

I. INTRODUCTION

Semiconductor nanowires have received a considerable interest over the past two decades as prime candidate for a new range of nanoscale building blocks with applications in electronics, photonics, quantum information technology, and research in fundamental physics. Nanowires possess major advantages over conventional thin film based structures. They can be grown by bottom up self-assembly to ensure a low cost production of high crystal quality devices. In addition, the radial strain relaxation in nanowires allows the growth of heterostructures whose constituent compounds are relatively lattice mismatched, hence providing a distinctive flexibility in terms of material composition. More recently, the growth of semiconductor nanowires without the use of heterocatalytic nanoparticle seeds has been the subject of intense research,[1–7] motivated by the potential of direct integration of nanowire devices with the established silicon CMOS technology.

In this context, arsenide and antimonide compounds such as InAs and InSb nanowires are of particular interest owing to their outstanding properties, including a very high mobility,[8–10] small effective mass, high spin-orbit coupling,[11] and large g-factor,[12,13] which make them suitable for spin-related applications such as quantum computation or observation of Majorana fermions in semiconductor/superconductor hybrid systems.[14] However, the absence of a heterocatalyst results in the nanowires displaying a large number of defects, as well as polytypism, i.e., uncontrolled axial modulation of the crystal structure between the zinc-blende (cubic) and the wurtzite (hexagonal) polytypes,[2,6] which in turn leads to a reduction of the electron mobility.[15] In a previous work, we investigated an approach to reduce the defect density in catalyst-free InAs nanowires via the incorporation of antimony during the growth.[16] The antimony incorporation suppresses the hexagonal phase and reduces the stacking fault (SF) density by up to one order of magnitude, resulting in a large increase in the electron mobility above that of pure InAs nanowires. For the development of future quantum electronic devices based on catalyst-free nanowires, it is of major importance to ensure that phase-coherent transport can be maintained over the length of the devices. Therefore, here we investigate the presence of phase coherent transport in catalyst-free InAs and InAs$_{1-x}$Sb$_x$ nanowires and estimate the phase coherence length in these nanowires.

At cryogenic temperatures, the transport properties of nanostructures become affected by quantum electron interference effects such as universal conductance fluctuations (UCFs) and localisation effects. Phase coherent transport can be observed when the dimensions of the structure are comparable to the phase coherence length l_Φ over which the phase coherence of the electrons is maintained. Owing to their small dimensions, semiconductor nanowires therefore constitute appropriate systems for the observation of fundamental quantum effects. In phase-coherent mesoscopic devices presenting a large number of electron channels, the conductance exhibits oscillations as a function of external parameters such as magnetic field or gate voltage. When travelling through the device, an electron is scattered many times and can acquire various phases corresponding to the different possible paths. The interference of the possible electron waves leads to a correction of the conductance. By varying the interference conditions, e.g., via the magnetic field or gate voltage as described below, it is possible to tune this correction therefore giving rise to universal conductance fluctuations (UCFs). UCFs have been observed in carbon nanotubes[17] and in various types of semiconductor nanowires, including InAs,[18–20] InN,[21–23] InSb,[24,25] GaN,[26] and indium tin oxide.[27] Another type of electron interference phenomenon is localisation. Weak localisation (WL) is due to the contribution of time-reversed electron paths to the quantum backscattering amplitude, giving rise to constructive interference and to a decrease of the conductance. In the presence of a magnetic field, electron waves following time-reversed paths acquire different phase shifts leading to a suppression of the conductance correction. A characteristic signature of the WL effect is therefore a positive differential magnetoconductance. Conversely, in the presence of strong

TABLE I. Average dimensions and electrical properties of the two groups of nanowires investigated. Mobility and carrier concentration are given at room-temperature (μ_{300K}, n_{300K}) and at 10 K (μ_{10K}, n_{10K}).

Material	Polytype	Diameter (nm)	SF density[a] (/μm)	Resistivity (Ω cm)	μ_{300K} (cm^2/ V s)	n_{300K} (cm^{-3})	μ_{10K} (cm^2/ V s)	n_{10K} (cm^{-3})
InAs	Wurtzite (83%)	90–160	360	0.006	350	2.2×10^{18}	1480	5.0×10^{17}
InAs$_{0.85}$Sb$_{0.15}$	Zinc-blende (99%)	95–120	35	0.01	1570	3.7×10^{17}	3750	1.6×10^{17}

[a]Stacking fault density.

spin-orbit coupling, the interference is destructive at zero field which leads to an increase of the conductance known as weak anti-localisation (WAL) effect.

Here, we investigate whether phase-coherent transport can be maintained in catalyst-free InAs and InAs$_{1-x}$Sb$_x$ nanowires and compare three different techniques to obtain information on the phase coherence length l_Φ from the study of electron interference effects at low temperature. We analyse aperiodic universal conductance fluctuations observed first by varying the magnetic field and then by changing the Fermi energy via the modulation of a back-gate voltage. Finally, we study the weak anti-localisation effect which can be clearly distinguished from the conductance fluctuations by averaging the magnetoconductance at different gate voltages. A phase coherence length in the hundred nanometre range is observed for all nanowires below 10 K. This is similar to the value obtained for Au-catalysed InAs nanowires. This demonstrates the potential of catalyst-free nanowires for future quantum electronic devices.

II. EXPERIMENTAL DETAILS

The study of coherent electron transport was performed on InAs and InAs$_{0.85}$Sb$_{0.15}$ nanowires grown by molecular beam epitaxy via a catalyst-free process, as described in a previous work.[16] Table I shows the average dimensions and electrical characteristics (extracted from field-effect measurements[16]) of the studied groups of nanowires. The mobility of the InAs$_{0.85}$Sb$_{0.15}$ nanowires is significantly higher than that of the InAs nanowires. Conversely, the InAs nanowires present a higher carrier concentration. The distribution of polytypes and defects in the nanowires was quantified through high-resolution TEM.[16] The InAs nanowires exhibit a mixture of wurtzite and zinc-blende structures with a dominant wurtzite polytype (83% of wurtzite polytype on average) and a high density of stacking faults (SF): 360 SF per micrometer. In contrast, the InAs$_{0.85}$Sb$_{0.15}$ nanowires display an almost pure zinc-blende phase (~99%) and a density of stacking faults reduced by one order of magnitude (35 SF per micrometer).

Electron beam lithography was used to attach metallic contacts (a bilayer of 3 nm Nb and 100 nm Au) on the nanowires. The separation between the two contacts varied from 200 to 600 nm. All contacts had a fixed width of 250 nm. Before the deposition of the contacts by sputtering, the contact area of the InAs and InAs$_{0.85}$Sb$_{0.15}$ nanowires was argon milled to remove the native oxide layer and ensure transparent contacts.[28] Figure 1(c) shows a typical nanowire device. Electrical characterisations were carried out by using a Keithley 4200-SCS semiconductor characterisation system.

The drain-source voltage V_{ds} was fixed to 100 μV for all nanowires. Low temperature magnetoconductance measurements were performed in a Physical Properties Measurement System (PPMS) manufactured by Quantum Design, allowing the control of magnetic fields up to ±13 T and a temperature range of 0.5–400 K. Measurements of the conductance were typically taken every 10 to 20 mT. The contribution of the noise due to the measurement system was estimated to correspond to an uncertainty of less than 5% in the determination of the phase coherence length l_Φ.

III. CONDUCTANCE FLUCTUATIONS: MAGNETIC FIELD

Information on the electron phase coherence length can be gained from the study of universal conductance fluctuations as a function of magnetic field or back-gate voltage. At low temperature, we find that the resistance R of a nanowire in a magnetic field applied perpendicular to its axis fluctuates upon variation of the magnetic field value. The extraction of the magnetoconductance $G_B = 1/R$ shows that the amplitude of the fluctuations is on the order of e^2/h, as seen in Figure 1(a). The magnetoconductance is typically symmetric upon field reversal for two-point measurements.[29,30] The conductance fluctuations are clearly distinguishable from noise by the fact that they are reproducible when the measurement is
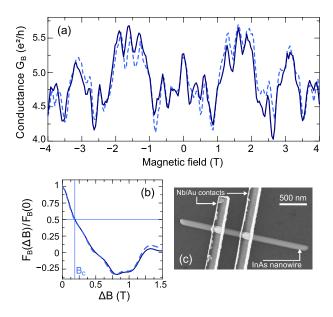

FIG. 1. (a) Typical plot of the normalised conductance G_B for an InAs nanowire as a function of magnetic field, first for a forward sweep (solid line) and then a backward sweep (dashed line) at T = 2 K. The magnetic field is perpendicular to the nanowire axis. (b) Corresponding autocorrelation functions showing the determination of B_c. (c) SEM image of an InAs nanowire connected by two Nb/Au contacts with 300 nm separation.

repeated on the same sample, as shown in Figure 1. Here, the fluctuations are measured for a single InAs nanowire, first for a forward sweep of the magnetic field from −4 to 4 T and then for a backward sweep. While UCFs are reproducible on a given sample, two macroscopically identical samples (i.e., of the same dimensions and material) will not give the same fluctuation pattern as the correction to the conductance depends on the precise arrangement of the scattering centres in the sample which determine the possible paths for the electrons.

The relative amplitude of the fluctuations can be studied by calculating the root mean square of the conductance: $\mathrm{rms}(G_B) = \sqrt{\mathrm{var}(G_B}$, where the variance is defined by $\mathrm{var}(x) = \langle (x - \langle x \rangle)^2 \rangle$ and $\langle ... \rangle$ is an average over the magnetic field. The electron phase coherence length l_Φ can be extracted from the correlation field B_c which quantifies the field scale above which the phase of the electrons has been randomised. B_c corresponds to the magnetic field at the half maximum of the autocorrelation function F of the magnetoconductance: $F(\Delta B) = \langle G_B(B + \Delta B)G_B(B) \rangle$ with ΔB a lag parameter in the magnetic field.[31] Figure 1(b) shows normalised autocorrelation functions from which is extracted B_c. Following a semi-classical approach, the correlation field B_c is inversely proportional to the maximum phase-coherently enclosed area $\mathcal{A}$ perpendicular to the field

$$B_c = \gamma \frac{\Phi_0}{\mathcal{A}}, \qquad (1)$$

where $\Phi_0 = h/e$ is the magnetic flux quantum and γ is a coefficient of order 1 which is estimated experimentally. For sufficiently low temperatures, the phase coherence length can exceed the contact separation L. In this case, for a magnetic field applied perpendicularly to the nanowire axis, we have $\mathcal{A} = Ld$, where d is the nanowire diameter. B_c reaches a saturation point $B_{c,sat}$ with respect to temperature, allowing the extraction of the γ coefficient: $\gamma = B_{c,sat}Ld/\Phi_0$. Otherwise, if $d < l_\Phi < L$, we have $\mathcal{A} = l_\Phi d$ and the phase coherence length l_Φ is extracted by using

$$B_c = \gamma \frac{\Phi_0}{l_\Phi d}. \qquad (2)$$

To get an estimation of γ, the temperature-dependence of conductance fluctuations was studied on a nanowire with a short contact separation. Figure 2(a) presents magnetoconductance measurements performed on an InAs nanowire with contacts separated by 235 nm for temperatures ranging between 0.5 and 25 K. As seen in Figure 2(b), the amplitude of the fluctuations remains approximately constant for temperatures up to 1.5 K before following a $T^{-0.25}$ decrease. Figure 2(c) shows the correlation field B_c as a function of temperature. Following a trend similar to $\mathrm{rms}(G_B)$, B_c exhibits a constant value of $B_{c,sat} \sim 0.14$ T up to a temperature of 2 K and then follows a $T^{0.22}$ increase. The presence of both the constant $\mathrm{rms}(G_B)$ and B_c demonstrates that the phase coherence length exceeds the contact separation below 2 K. This gives a value of 1.1 for the γ coefficient which will be used in the following to estimate the phase coherence length
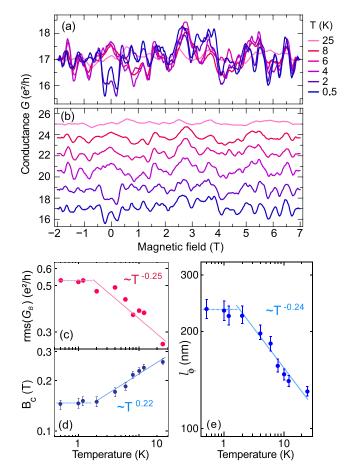

FIG. 2. (a) Fluctuating magnetoconductance of an InAs nanowire (sample A) at various temperatures. (b) The same fluctuations, vertically shifted for clarity. (c) Root-mean-square and (d) correlation field B_c of the magnetoconductance as a function of temperature. The error bars for B_c correspond to the spacing in magnetic field between two consecutive measurement points. (e) Temperature-dependence of the phase-coherence length. The magnetic field was applied perpendicular to the nanowire axis. Dots are experimental data points. Solid lines represent power law fits.

of the nanowires. This value is consistent with the 0.95–2.0 range reported in the literature for InAs nanowires.[32–34]

The phase coherence length was extracted for a series of InAs and InAs$_{0.85}$Sb$_{0.15}$ nanowires. The results corresponding to some of the studied nanowires are summarised in Table II. At 2 K, B_c varies from 0.12 to 0.28 T from one sample to another. This corresponds to phase coherence lengths in the 240–300 nm range for the InAs nanowires and in the

TABLE II. Dimensions and characteristics of the InAs and InAs$_{0.85}$Sb$_{0.15}$ nanowires investigated. The values of B_c, $\mathrm{rms}(G_B)$ and l_Φ are given at a temperature of 2 K. L is the contact separation and d the nanowire diameter. The magnetic field was oriented perpendicular to the nanowire axis.

Sample	Material	L (nm)	d (nm)	B_c (T)	$\mathrm{rms}\,(G_B)(e^2/h)$	l_Φ (nm)
A	InAs	235	135	0.14	0.48	235
B	InAs	396	114	0.13	0.40	300
C	InAs	480	160	0.12	0.50	240
D	InAs	525	120	0.15	0.34	255
E	InAs	570	110	0.17	0.49	240
F	InAsSb[a]	530	120	0.28	0.70	135
G	InAsSb[a]	523	95	0.23	0.49	210

[a]InAs$_{0.85}$Sb$_{0.15}$.

135–210 nm range for the $InAs_{0.85}Sb_{0.15}$ nanowires, which is similar to typical values reported in the literature for III–V semiconductor nanowires[24,35] and for Au-catalysed InAs nanowires.[18] We note that despite their major structural differences, the phase coherence length is of the same order for both InAs and $InAs_{0.85}Sb_{0.15}$ nanowires. This can be explained by the fact that rigid scatterers do not contribute to the loss of phase coherence.[36]

IV. CONDUCTANCE FLUCTUATIONS: GATE VOLTAGE

Gate voltage-dependent measurements constitute an alternative way to observe universal conductance fluctuations. A change in gate voltage V_g leads to a variation of the electron Fermi energy which is equivalent to a re-arrangement in energy of the scattering centres. This causes electrons to travel through different transport channels and to acquire a different phase shift, hence the fluctuation of the conductance. Contrary to magnetoconductance fluctuations which are symmetric upon field reversal, gate voltage induced fluctuations are not expected to be symmetric with respect to V_g. Typical conductance fluctuation patterns obtained for a gate voltage sweep at zero magnetic field on an $InAs_{0.85}Sb_{0.15}$ nanowire (sample G) are presented in Figure 3(a) for a range of temperatures. Following the general n-type semiconductor behaviour, the average conductance increased as a function of gate voltage
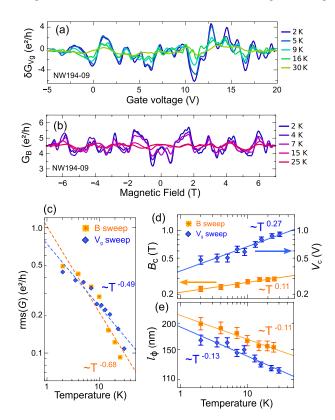

FIG. 3. Conductance in units of e^2/h as a function of: (a) gate voltage at $B = 0$ T and (b) magnetic field (perpendicular orientation) for a fixed $V_g = 0$ V. The measurements were performed on an $InAs_{0.85}Sb_{0.15}$ nanowire (sample G) for temperatures ranging from 2 to 30 K. (c) Root-mean-square of the conductance fluctuations obtained for both B and V_g sweeps as a function of temperature. (d) Correlation field B_c and correlation voltage V_c as a function of temperature. (e) Temperature-dependence of the phase coherence length l_Φ for both B and V_g sweeps. Dashed and solid lines represent fits to the experimental data.

due to the change in electron concentration. To isolate the conductance fluctuations from this macroscopic effect, the slowly varying background was estimated by a second-order polynomial fit[18] and then subtracted from the raw data to obtain the conductance oscillations $\delta G(V_g)$ presented in Figure 3(a). As a comparison, conductance fluctuations obtained for a magnetic field sweep (perpendicular orientation) on the same nanowire at zero gate voltage are displayed in Figure 3(b). In both cases, the amplitude of the fluctuations is on the order of e^2/h and decreases with increasing temperature as illustrated in Figure 3(c). The decrease of rms(G_B) and rms(G_{V_g}) is proportional to $T^{-0.68}$ and $T^{-0.49}$, respectively.

Similarly to the magnetoconductance measurements, the electron phase coherence length can be determined from the correlation voltage V_c which quantifies the voltage scale above which the change of the Fermi energy is large enough to give rise to an uncorrelated value of the conductance.[31] V_c is the voltage obtained at the half maximum of the autocorrelation function of the conductance $\delta G(V_g)$. An estimation for l_Φ as a function of the correlation voltage V_c was developed by Petersen *et al.*[22] for InN nanowires presenting a two-dimensional accumulation layer at the surface. By adapting this estimation to InAs and $InAs_{1-x}Sb_x$ nanowires presenting three-dimensional transport, we obtain

$$l_\Phi = \sqrt{\frac{4\pi m^* \mathcal{D}}{\hbar (3\pi^2 n_{3d})^{2/3} \left[\left(1 - \frac{V_c}{V_{th}}\right)^{2/3} - 1 \right]}}. \tag{3}$$

Here, $\hbar$ is the reduced Planck constant, m^* is the electron effective mass, $\mathcal{D}$ is the diffusion length, n_{3d} is the carrier concentration of the nanowire, and V_{th} is the threshold voltage, extracted from field-effect measurements. When $V_c \ll V_{th}$, this simplifies into

$$l_\Phi = \sqrt{\frac{h V_{th} \mu}{e V_c}}, \tag{4}$$

where μ is the electron mobility, also extracted from field-effect measurements. As seen in Figure 3(d), both the correlation field B_c and the correlation voltage V_c increase as a function of temperature which corresponds to a decrease of the phase coherence length l_Φ. It should be noted that the temperature-dependent decays of l_Φ obtained by either magnetic field measurements or gate voltage measurements are very similar, as shown in Figure 3(e). At 2 K, we obtain $l_{\Phi,B} = 210$ nm for the B sweep and $l_{\Phi,V_g} = 170$ nm for the V_g sweep. These values are in relatively good agreement given the uncertainty in the determination of both $l_{\Phi,B}$ (due to the estimation of the γ coefficient) and $l_{\Phi V_g}$ (due to the relatively short separation between the contacts to the nanowire which could lead to an underestimation of the electron mobility[37]). Magnetic field measurements and gate voltage measurements therefore appear to be two consistent approaches for the extraction of the phase coherence length.

V. LOCALISATION EFFECTS

The analysis of localisation effects, such as weak localisation (WL) or weak anti-localisation (WAL), represents an

additional approach to gain information on the phase coherence length. However, the presence of universal conductance fluctuations in single nanowires may prevent the observation of these effects. Two different methods to reveal distinguishable localisation features in semiconductor nanowires have been reported. The first one is to connect several nanowires in parallel in order to attenuate the conductance fluctuation amplitude.[19,21] The second one, investigated here, consists of smoothing the fluctuations by averaging the magnetoconductance of a single nanowire measured at different fixed back-gate voltages.[21] This method requires that l_Φ be independent of V_g.

A set of magnetoconductance measurements was performed on single InAs and InAs$_{0.85}$Sb$_{0.15}$ nanowires for fixed back-gate voltages between 0 and 30 V. Figure 4(a) shows the magnetoconductance measurements for an InAs nanowire at a temperature of 2 K for a selection of gate voltages. The magnetoconductance correction ΔG, as seen in Figure 4(b), is obtained after averaging all the single magnetoconductance traces taken at different gate voltages. By comparison with the single magnetoconductance traces, ΔG exhibits a considerable damping of the fluctuations with a decrease in the amplitude by a factor 2.5. However, the fluctuation amplitude of ΔG remains approximately three times higher than the noise level of the measurement system (not shown here). ΔG features a small distinguishable peak at zero magnetic field which represents a possible signature of weak anti-localisation due to the presence of spin-orbit coupling, as investigated below. The correlation field was extracted for each magnetoconductance trace to study the dependence of the phase coherence length on the gate voltage V_g. As illustrated in Figure 4(c), l_Φ remains stable over the whole range of measurements and appears to be independent (to within the accuracy of measurement) of the applied gate voltage. This experiment was repeated on several InAs and InAs$_{0.85}$Sb$_{0.15}$ nanowire devices. For each nanowire, the value of l_Φ was found to be independent of V_g.

From the average mobility and carrier concentration given in Table I, we estimate the elastic mean free path l_m of the nanowires to be in the range 20–50 nm at the investigated temperature of 2 K. The diameter d of all studied nanowires being larger than 95 nm, we can consider that the nanowire samples are in the "dirty" limit of the diffusive regime (i.e., $l_m < d$). The averaged magnetoconductance correction should therefore follow[38–40]

$$\Delta G_B = G_0 - \frac{2e^2}{hL}\left[\frac{3}{2}\left(\frac{1}{l_\Phi^2} + \frac{4}{3l_{so}^2} + \frac{1}{l_B^2}\right)^{-\frac{1}{2}} - \frac{1}{2}\left(\frac{1}{l_\Phi^2} + \frac{1}{l_B^2}\right)^{-\frac{1}{2}}\right],$$
(5)

where G_0 is the value of the magnetoconductance at zero magnetic field, l_{so} is the spin-orbit scattering length, and l_B is the magnetic relaxation length, the expression for which depends on the orientation of the magnetic field with respect to the nanowire axis: $l_B = \hbar\sqrt{3}/(eBd)$ for a perpendicular magnetic field and $l_B = \hbar\sqrt{2\pi}/(eBd)$ for a parallel magnetic field. This expression is only valid when the magnetic length $l_M = \sqrt{\hbar/(eB)}$ exceeds the nanowire diameter d.

Figure 5 shows the magnetoconductance curves obtained after averaging over the gate voltage for an InAs nanowire (Figure 5(a)) and an InAs$_{0.85}$Sb$_{0.15}$ nanowire (Figure 5(b)). The nanowires have a diameter of 110 nm and 95 nm, respectively. Therefore, in order to satisfy the condition $l_M > d$, the fitting of the experimental data points to Equation (5) was restricted to small magnetic fields with $|B| < 0.05$ T for the InAs nanowire (sample E) and $|B| < 0.07$ T for the InAs$_{0.85}$Sb$_{0.15}$ nanowire (sample G). At zero magnetic field, we observe a clear conductance peak due to weak anti-localisation effects. By fitting the experimental data to Equation (5), it is possible to estimate the values of both l_Φ and l_{so}. We extract a phase coherence length l_Φ of 195 and 170 nm for the InAs and InAs$_{0.85}$Sb$_{0.15}$ nanowires, respectively. As a comparison, the values of l_Φ obtained via the correlation field from the observation of UCFs were, respectively, 240 and 210 nm for the same nanowires. Both the WAL model and UCF model describe the phase coherence length reasonably, with a difference of less than 20% between the two models. Although spin-orbit interactions are
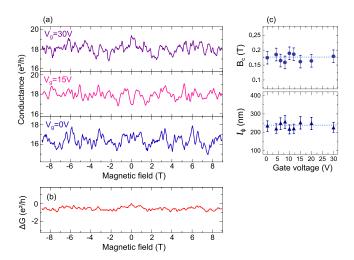

FIG. 4. (a) Magnetoconductance G for an InAs nanowire (sample E) measured at 2 K for gate voltages V_g ranging from 0 to 30 V. (b) Magnetoconductance correction ΔG averaged over the different gate voltages. The magnetoconductance correction is offset to zero at zero magnetic field. (c) Correlation field B_c and phase coherence length l_Φ as a function of the applied gate voltage. The dashed lines represent the average value of B_c and l_Φ.
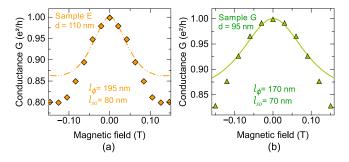

FIG. 5. Magnetoconductance fluctuations averaged over the gate voltage for two different nanowires: (a) an InAs nanowire (sample E) in perpendicular magnetic field and (b) an InAs$_{0.85}$Sb$_{0.15}$ nanowire (sample G) in parallel magnetic field. The magnetoconductance is offset to e^2/h at zero magnetic field. Symbols are experimental data. Lines represent fits to Equation (5) restricted to $|B| < 0.05$ T for Figure (a) and $|B| < 0.07$ T for Figure (b). The extracted values of l_Φ and l_{so} are indicated in the figures. The measurements were performed at 2 K.

not the main focus of this analysis, we can also extract spin-relaxation lengths l_{so} of 80 nm and 70 nm for the InAs nanowire and InAs$_{0.85}$Sb$_{0.15}$ nanowire, respectively. They are in close agreement with values previously reported for InAs nanowires.[32,41]

VI. CONCLUSION

We have studied three different quantum interference effects to assess phase-coherent transport in catalyst-free nanowires at cryogenic temperatures and to gain information on the electron phase coherence length l_Φ of our InAs and InAs$_{1-x}$Sb$_x$ nanowires. We first investigated universal conductance fluctuations obtained by varying either the magnetic field or the back-gate voltage. We then observed anti-localisation effects obtained by averaging the magneto-conductance of single nanowires measured at different back-gate voltages. The analysis of these three electron interference effects gave very consistent results with a variation of less than 20% between the models. Despite the relatively high number of defects in the catalyst-free InAs nanowires, we estimated a phase-coherence length in the hundred nanometre range for both InAs and InAs$_{1-x}$Sb$_x$ nanowires at 2 K which is similar to values obtained for Au-catalysed nanowires. The observation of phase coherent transport in catalyst-free nanowires unlocks new possibilities to exploit coherent phenomena in future nanowire-based quantum electronics directly integrated with silicon CMOS technology.

ACKNOWLEDGMENTS

[1] B. Mandl, J. Stangl, E. Hilner, A. A. Zakharov, K. Hillerich, A. W. Dey, L. Samuelson, G. Bauer, K. Deppert, and A. Mikkelsen, Nano Lett. **10**, 4443 (2010).

[2] B. Mandl, J. Stangl, T. Mårtensson, A. Mikkelsen, J. Eriksson, L. S. Karlsson, G. Bauer, L. Samuelson, and W. Seifert, Nano Lett. **6**, 1817 (2006).

[3] G. Koblmüller, S. Hertenberger, K. Vizbaras, M. Bichler, F. Bao, J.-P. Zhang, and G. Abstreiter, Nanotechnology **21**, 365602 (2010).

[4] L. Gao, R. L. Woo, B. Liang, M. Pozuelo, S. Prikhodko, M. Jackson, N. Goel, M. K. Hudait, D. L. Huffaker, M. S. Goorsky, S. Kodambaka, and R. F. Hicks, Nano Lett. **9**, 2223 (2009).

[5] Y. Zhang, M. Aagesen, J. V. Holm, H. I. Jørgensen, J. Wu, and H. Liu, Nano Lett. **13**, 3897 (2013).

[6] W. Wei, X.-Y. Bao, C. Soci, Y. Ding, Z.-L. Wang, and D. Wang, Nano Lett. **9**, 2926 (2009).

[7] I. Isakov, M. Panfilova, M. J. L. Sourribes, V. Tileli, A. E. Porter, and P. A. Warburton, Nanotechnology **24**, 085707 (2013).

[8] B. P. Tinkham, B. R. Bennett, R. Magno, B. V. Shanabrook, and J. B. Boos, J. Vacuum Sci. Technol. B **23**, 1441 (2005).

[9] V. W. L. Chin, R. J. Egan, and T. L. Tansley, J. Appl. Phys. **69**, 3571 (1991).

[10] O. Gül, D. J. van Woerkom, I. van Weperen, D. Car, S. R. Plissard, E. P. A. M. Bakkers, and L. P. Kouwenhoven, Nanotechnology **26**, 215202 (2015).

[11] S. Nadj-Perge, V. S. Pribiag, J. W. G. van den Berg, K. Zuo, S. R. Plissard, E. P. A. M. Bakkers, S. M. Frolov, and L. P. Kouwenhoven, Phys. Rev. Lett. **108**, 166801 (2012).

[12] I. Vurgaftman, J. R. Meyer, and L. R. Ram-Mohan, J. Appl. Phys. **89**, 5815 (2001).

[13] J. Kammhuber, M. C. Cassidy, H. Zhang, O. Gül, F. Pei, M. W. A. de Moor, B. Nijholt, K. Watanabe, T. Taniguchi, D. Car, S. R. Plissard, E. P. A. M. Bakkers, and L. P. Kouwenhoven, Nano Lett. **16**, 3482 (2016).

[14] V. Mourik, K. Zuo, S. M. Frolov, S. R. Plissard, E. P. A. M. Bakkers, and L. P. Kouwenhoven, Science **336**, 1003 (2012).

[15] C. Thelander, P. Caroff, S. Plissard, A. W. Dey, and K. A. Dick, Nano Lett. **11**, 2424 (2011).

[16] M. J. L. Sourribes, I. Isakov, M. Panfilova, H. Liu, and P. A. Warburton, Nano Lett. **14**, 1643 (2014).

[17] H. T. Man and A. F. Morpurgo, Phys. Rev. Lett. **95**, 026801 (2005).

[18] Y. Doh, A. L. Roest, E. P. A. M. Barkers, S. De Franceschi, and L. P. Kouwenhoven, J. Korean Phys. Soc. **54**, 135 (2009).

[19] A. E. Hansen, M. T. Björk, C. Fasth, C. Thelander, and L. Samuelson, Phys. Rev. B **71**, 205328 (2005).

[20] T. S. Jespersen, M. Aagesen, C. Sørensen, P. E. Lindelof, and J. Nygård, Phys. Rev. B **74**, 233304 (2006).

[21] S. Alagha, S. E. Hernández, C. Blömers, T. Stoica, R. Calarco, and T. Schäpers, J. Appl. Phys. **108**, 113704 (2010).

[22] G. Petersen, S. E. Hernández, R. Calarco, N. Demarina, and T. Schäpers, Phys. Rev. B **80**, 125321 (2009).

[23] R. Frielinghaus, S. E. Hernández, R. Calarco, and T. Schäpers, Appl. Phys. Lett. **94**, 252107 (2009).

[24] H. Yao, H. Yusuf Gnel, C. Blmers, K. Weis, J. Chi, J. Grace Lu, J. Liu, D. Grützmacher, and T. Schäpers, Appl. Phys. Lett. **101**, 082103 (2012).

[25] I. van Weperen, B. Tarasinski, D. Eeltink, V. S. Pribiag, S. R. Plissard, E. P. A. M. Bakkers, L. P. Kouwenhoven, and M. Wimmer, Phys. Rev. B **91**, 201413 (2015).

[26] M. T. Elm, P. Uredat, J. Binder, L. Ostheim, M. Schäfer, P. Hille, J. Mübener, J. Schörmann, M. Eickhoff, and P. J. Klar, Nano Lett. **15**, 7822 (2015).

[27] P.-Y. Yang, L. Y. Wang, Y.-W. Hsu, and J.-J. Lin, Phys. Rev. B **85**, 085423 (2012).

[28] M. J. L. Sourribes, I. Isakov, M. Panfilova, and P. A. Warburton, Nanotechnology **24**, 045703 (2013).

[29] M. Buttiker, IBM J. Res. Dev. **32**, 317 (1988).

[30] L. Onsager, Phys. Rev. **38**, 2265 (1931).

[31] P. A. Lee, A. D. Stone, and H. Fukuyama, Phys. Rev. B **35**, 1039 (1987).

[32] S. Estévez Hernández, M. Akabori, K. Sladek, C. Volk, S. Alagha, H. Hardtdegen, M. G. Pala, N. Demarina, D. Grützmacher, and T. Schäpers, Phys. Rev. B **82**, 235303 (2010).

[33] C. Blömers, M. I. Lepsa, M. Luysberg, D. Grützmacher, H. Luth, and T. Schäpers, Nano Lett. **11**, 3550 (2011).

[34] R. Frielinghaus, K. Flöhr, K. Sladek, T. E. Weirich, S. Trellenkamp, H. Hardtdegen, T. Schäpers, C. M. Schneider, and C. Meyer, Appl. Phys. Lett. **101**, 062104 (2012).

[35] C. Blömers, J. G. Lu, L. Huang, C. Witte, D. Grützmacher, H. Lüth, and T. Schäpers, Nano Lett. **12**, 2768 (2012).

[36] S. Datta, *Electronic Transport in Mesoscopic Systems* (Cambridge University Press, 1997).

[37] O. Wunnicke, Appl. Phys. Lett. **89**, 083102 (2006).

[38] C. Kurdak, A. M. Chang, A. Chin, and T. Y. Chang, Phys. Rev. B **46**, 6846 (1992).

[39] C. W. J. Beenakker and H. van Houten, Phys. Rev. B **38**, 3232 (1988).

[40] P. A. Lee and T. V. Ramakrishnan, Rev. Mod. Phys. **57**, 287 (1985).

[41] S. Dhara, H. S. Solanki, V. Singh, A. Narayanan, P. Chaudhari, M. Gokhale, A. Bhattacharya, and M. M. Deshmukh, Phys. Rev. B **79**, 121311 (2009).